Biomaterials 35 (2014) 304–315

Contents lists available at ScienceDirect

Biomaterials

journal homepage: www.elsevier.com/locate/biomaterials

Peptide-based MRI contrast agent and near-infrared fluorescent probe for intratumoral legumain detection

Yu-Jen Chen [a], Shou-Cheng Wu [a], Chung-Yung Chen [b], Shey-Cherng Tzou [a], Tian-Lu Cheng [c], Ying-Fang Huang [a], Shyng-Shiou Yuan [d,**], Yun-Ming Wang [a,c,*]

[a] Department of Biological Science and Technology, National Chiao Tung University, 75 Bo-Ai Street, Hsinchu 300, Taiwan
[b] Department of Bioscience Technology, Chung Yuan Christian University, Chungli 320, Taiwan
[c] Department of Biomedical Science and Environmental Biology, Kaohsiung Medical University, Kaohsiung 807, Taiwan
[d] Translational Research Center, Cancer Center, and Department of Obstetrics and Gynecology, Kaohsiung Medical University Hospital, Kaohsiung Medical University, Kaohsiung 807, Taiwan

ARTICLE INFO

Article history:
Received 6 September 2013
Accepted 25 September 2013
Available online 10 October 2013

Keywords:
Legumain
MRI
Optical imaging
Contrast agent

ABSTRACT

Recent studies suggest that intratumoral legumain promotes tumorigenesis. To monitor legumain activity in tumors, we developed a new MRI contrast agent ([Gd-NBCB-TTDA-Leg(L)]) and a NIR fluorescence probe (CyTE777-Leg(L)-CyTE807). The MRI contrast agent was prepared by introduction of cyclobutyl and benzyl group residues to TTDA (3,6,10-tri(carboxymethyl)-3,6,10-triaza-dodecanedioic acid), followed by the attachment of a legumain-specific substrate peptide (Leg(L)). The NIR fluorescence probe was designed by conjugating two NIR fluorochromes (CyTE777 and CyTE807) with Leg(L). Peptide cleavage of the MRI contrast agent by legumain can increase its hydrophobicity and promote rotational correlation time (τ_R). Peptide cleavage of the NIR probes by the legumain relieves the self quench of the probe. Peptide cleavage of the MRI contrast agent and the NIR fluorescence probe by legumain were confirmed by T_1 relaxometric studies and by fluorescence studies, respectively. *In vivo* MR images showed that [Gd-NBCB-TTDA-Leg(L)] attained 55.3 fold (254.2% versus 4.6%, at 2.0 h post-injection) higher imaging enhancement, as compared with control contrast agent bearing a noncleaveable peptide ([Gd-NBCB-TTDA-Leg(D)], in the CT-26 (legumain$^+$) tumors. Similarly, optical imaging probe CyTE777-Leg(L)-CyTE807 attained 15.2 fold (3.34×10^9 photons/min versus 0.22×10^9 photons/min, at 24.0 h post-injection) higher imaging enhancement in the CT-26 (legumain$^+$) tumors, compared to a NIR control probe (CyTE777-Leg(D)-CyTE807). These data indicate that the [Gd-NBCB-TTDA-Leg(L)] and the CyTE777-Leg(L)-CyTE807 probes may be promising tools to image the legumain-expressing cancers for diagnoses and targeted treatments.

1. Introduction

Magnetic resonance imaging (MRI) is one of the most important tools for cancer diagnosis, and its imaging effect depends upon the combination of MRI contrast agents and the density of water molecules in the body. Advances in MRI have extended the application of this technology from clinical diagnosis to routine cellular imaging [1–3]. Hence, many interdisciplinary researchers have been interested in developing more efficient MRI contrast agents for targeting MR imaging.

Many studies have reported the use of lactoferrin [4], folic acid [5–7], peptide, [8,9] nucleic acid [10], and monoclonal antibodies [11,12] as targeting components of MRI contrast agents. Receptor-mediated endocytosis [13] of these conjugated MRI contrast agents provides an efficient and specific tumor targeting and imaging. On the other hand, optical imaging techniques has been established as a powerful tool for *in vitro* and *in vivo* molecular imaging for its superior sensitivity and selectivity [14,15]. In this settings, near-infrared (NIR) fluorochromes are more widely used than fluorochromes with visible spectra since the excitation/emission of NIR (650–900 nm) can penetrate deep tissues without been absorbed by the blood [16,17]. Use of NIR optical imaging has become increasingly attractive to biological scientists due to low

* Corresponding author. Department of Biological Science and Technology, National Chiao Tung University, 75 Bo-Ai Street, Hsinchu 300, Taiwan. Tel.: +886 3 5712121x56972; fax: +886 3 5729288.
** Corresponding author. Tel.: +886 7 3121101x2555.
E-mail addresses: yuanssf@ms33.hinet.net (S.-S. Yuan), ymwang@mail.nctu.edu.tw (Y.-M. Wang).

0142-9612/$ – see front matter © 2013 Elsevier Ltd. All rights reserved.
http://dx.doi.org/10.1016/j.biomaterials.2013.09.100

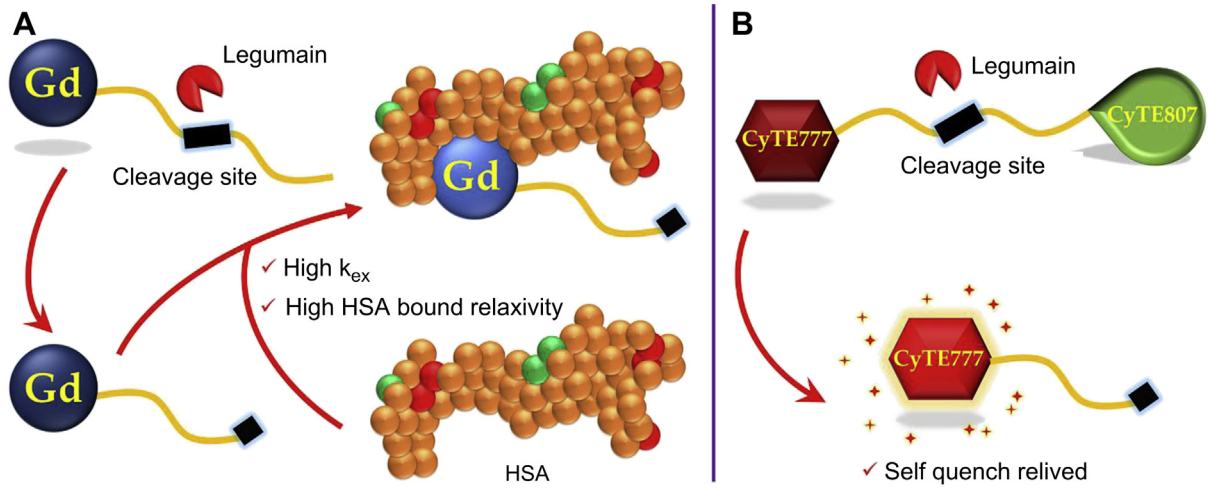

Fig. 1. Systematic representation of (A) MRI contrast agent ([Gd-NBCB-TTDA-Leg(L)]) and (B) NIR fluorescent probe (CyTE777-Leg(L)-CyTE807) for legumain detection.

auto fluorescence, low phototoxicity and deep tissue penetration [18–20]. Proteases participate in tumor formation, angiogenesis, local invasion, and metastatic spread [21–23]. Therefore, proteases may be promising targets for developments of anticancer drugs that act preferentially at cancer sites. In line with this notion, several protease inhibitors, such as the MMP inhibitors marimastat [24], AG3340 [25], S-3304 [26], and BAY 12-9566, [27] have entered phase I, II, and III clinical trials for cancer therapy for colon cancers.

Many studies have clearly revealed the correlation between protease expression and poor prognosis in patients with cancer, [28] indicating that proteases may also be used as markers to predict tumor recurrence and prognostic survival. Thus, tumor-associated proteases seem attractive as both therapeutic targets and prognosis markers. Therefore, the technology to image protease activity *in vivo* would provide a valuable tool to design personalized, protease activity-based prodrug therapies and to monitor tumor recurrences and patient prognoses. Based on these recent developments, we chose legumain (Leg) as a target in this study. Legumain or asparaginly endopeptidase (AEP) is a lysosomal cysteine protease with a high cleavage specificity after an asparagine residue of substrate proteins [29,30]. Legumain expression and activity are linked to a number of pathological conditions including cancer, atherosclerosis, and inflammation, yet its biological role in these pathologies is not well-understood. It is over-expressed in a majority of human solid tumors such as carcinomas of the breast, colon, and prostate. Knock-down of legumain in mouse cancer models results in marked decrease in tumor growth and metastasis [29]. Several macromolecular substrates have been identified for legumain including MMP-2, [31] cathepsins H, B, L, [32] thymosin [33], and fibronectin [34]. Highly potent and selective inhibitors for legumain would not only be valuable for functional studies of legumain in these conditions, but also useful for therapies as well. In addition, development of imaging probes capable of detecting legumain activity is likely to aid in tumor diagnosis and treatments.

In this study, we designed and synthesized a new MRI contrast agent ([Gd-NBCB-TTDA-Leg(L)]) and a NIR fluorescent probe (CyTE777-Leg(L)-CyTE807) for *in vitro* and *in vivo* detection of legumain activity. A cyclobutyl and a benzyl group residues were introducted on the carbon backbone of TTDA (3,6,10-tri(carboxymethyl)-3,6,10-triaza-dodecanedioic acid) to increase lipophilicity to the Gd(III) complex upon cleavage of a legumain-specific peptide substrate (Leg(L)) linked to the benzyl group. Legumain-mediated cleavage of the peptide substrate thus facilitate better wrapping of the Gd(III) ion and increases the water exchange rate (k_{ex}). The CyTE777-Leg(L)-CyTE807 was created by conjugating two NIR fluorochromes (CyTE777 and CyTE807) to Leg(L). In close proximity, emission from CyTE777 is expected to transfer to CyTE807, thus quench CyTE777 signals. We postulated that enzymatic removal of the peptide substrate of [Gd-NBCB-TTDA-Leg(L)], followed by binding with HSA would eventually lead to the formation of macromolecules. On the other hand, enzymatic removal of the peptide substrate of CyTE777-Leg(L)-CyTE807 would increase the distance between these two fluorochromes, and unveil the NIR fluorescent emission from CyTE777 (Fig. 1). The MRI contrast agent and the NIR fluorescent probe were evaluated by *in vitro* and *in vivo* MR imaging and optical imaging, respectively. A nude mice model bearing subcutaneous tumor xenografts of CT-26 (legumain^{+}) tumor was used for both MR and optical imaging studies.

2. Experimental

2.1. Materials and methods

Ninhydrin and palladium/charcoal (10% Pd) were purchased from Merck (Dietikon, Switzerland). O-(7-Aza-1H-benzotrlazol-1-yl)-N,N,N′,N′-tetramethyluronlum (HATU), N-methylmorpholine, trifluoroacetic acid (TFA), N-ethyldiisopropylamine, magnesium sulfate anhydrous, N-methyl morpholine, and N,N′-dicyclohexylcarbodiimide (DCC) were purchased from Alfa Aesar (Ward Hill, US). Triethylsilane (TIS), acetic anhydride, and hydrazine monohydrate were purchased from Acros (Fair Lawn, US). Borane tetrehydrofuran complex solution in THF (BH_3-THF), cyclobutane-1,1-dicarboxamide, succinic anhydride, thionyl chloride ($SOCl_2$), 3-mercaptopropionic acid, and Dulbecco's minimal essential medium were purchased from Sigma–Aldrich (St. Louis, US). Fmoc-Ala, Fmoc-(L)-Asn(Trt), Fmoc-Lys(Boc), Fmoc-Lys(ivDde), Fmoc-(D)-Asn(Trt), Fmoc-Leu, rink amide resin (200–400 mesh), N-hydroxybenzotriazole (HOBT), and benzotriazole-1-yl-oxy-tris-pyrrolidino-phosphoniumhexafluoro-phosphate (PyBOP) were purchased from Novabiochem (Nottingham, UK). N-methyl-2-pyrrolidinone (NMP) was purchased from Mallinckrodt Baker (Phillipsburg, US). All other chemicals and reagents for the synthesis and biological studies were of high quality and procured commercially from the reputed suppliers. The peptide synthesis was performed on PS-3 (Ridgefield, NJ, US). The 1H NMR and ^{13}C NMR spectra of the compounds were recorded in deuterated water (D_2O)/deuterated dimethulsulphoxide (DMSO-d_6) at room temperature using tetramethylsilane as an external standard on a Unity-300 NMR spectrometer (Varian, CA, US). LC-MS analyses were performed with Micromass ZQ-4000 and Q-Tof (Waters, MA, US). HPLC analysis was performed on AKTA basic 10 system (Amersham-Pharmacia, NJ, US) equipped with an UV-900 detector, Frac-920 fraction collector and RP-C18 column (5 μm, 4.6 × 250 mm) (Supelco, PA, US), eluted at a flow rate of 1 mL/min with a solvent system consisting of 0.1% TFA/H_2O (solvent B) and TFA/CH_3CN (solvent A). UV/Vis and fluorescence spectra were measured with U-3010 UV/Vis spectrophotometer (Hitachi, Tokyo, Japan) and F-9000 fluorescence spectrophotometer (Hitachi, Tokyo, Japan) at room temperature, respectively. The relaxation time (T_1) measurements were performed using NMS-120 Minispec relaxometer (Bruker, Ettlingen, Germany) operating at 20 MHz and 37.0 ± 0.1 °C.

In vitro and *in vivo* MR imaging was recorded on 7.0-T Biospec MR scanner (Bruker, Ettlingen, Germany) with a volume coil used as radio frequency transmitter and receiver. *In vitro* and *in vivo* optical images were acquired using IVIS Spectrum System (Caliper, MA, US).

2.2. Synthesis

Syntheses of peptide substrate (Fmoc-Leu-(L)-Asn(Trt)-Ala-Ala-Lys(Boc)-Lys(Boc)-Lys(Boc)-Lys(ivDde), Leg(L) and Fmoc-Leu-(D)-Asn(Trt)-Ala-Ala-Lys(Boc)-Lys(Boc)-Lys(Boc)-Lys(Boc)-Lys(ivDde), Leg(D)) [35].

The solid-phase peptide assembled on PS-3 peptide synthesizer was synthesized using rink amide resin (0.63 mmol/g) by Fmoc chemistry. The side chain protecting groups of trifunctional amino acids were trifluoroacetic acid labile. Legumain peptide substrate (Fmoc-Leu-(L)-Asn(Trt)-Ala-Ala-Lys(Boc)-Lys(Boc)-Lys(Boc)-Lys(ivDde), Leg(L)) was synthesized on a 0.16 mmol scale using a 4-fold molar excess of Fmoc-protected amino acids (0.62 mmol), which were activated by 4-fold excess of PyBOP in the presence of *N*-methyl morpholine (20% v/v) in DMF. N^{α} -Fmoc protecting groups were removed by treating the resin-attached peptide with piperidine (20% v/v) in DMF. The legumain functionalized resin (0.25 g, 0.16 mmol) was deprotected with the piperidine solution and washed in DMF as described above. The collected fractions yielded legumain peptide substrate as a green powder (253 mg, 85.8%). ESI-MS *m/z* calcd for $C_{41}H_{51}N_2O_8S_3$: 899.14, found: 899.61 $[M + H]^+$. The control legumain peptide substrate (Fmoc-Leu-(D)-Asn(Trt)-Ala-Ala-Lys(Boc)-Lys(Boc)-Lys(Boc)-Lys(ivDde), Leg(D)) was synthesized by following the steps as mentioned for Leg(L) by utilizing D-form asparagine as reaction substrate. The collected fractions yielded legumain peptide substrate as a green powder (241 mg, 81.7%). ESI-MS *m/z* calcd for $C_{41}H_{51}N_2O_8S_3$: 899.14, found: 899.83 $[M + H]^+$.

The details of the synthesis of compounds **1** to **6**, **11**, and **12** are reported in the Supporting Information, (Schemes S1† and S2†), and compounds **7** to **10**, and **13** to **14** are depicted in Schemes 1 and 2. The procedures are described as below.

2.2.1. Syntheses of NBCB-TTDA-Leg(L) (**7**) and NBCB-TTDA-Leg(D) (**8**)

In order to expose the *N*-terminal of peptide, the resin (0.5 g, 0.20 mmol) was soaked in NMP (2 mL) for 1 h. At the same time, HATU (120 mg, 0.32 mmol)/DMF

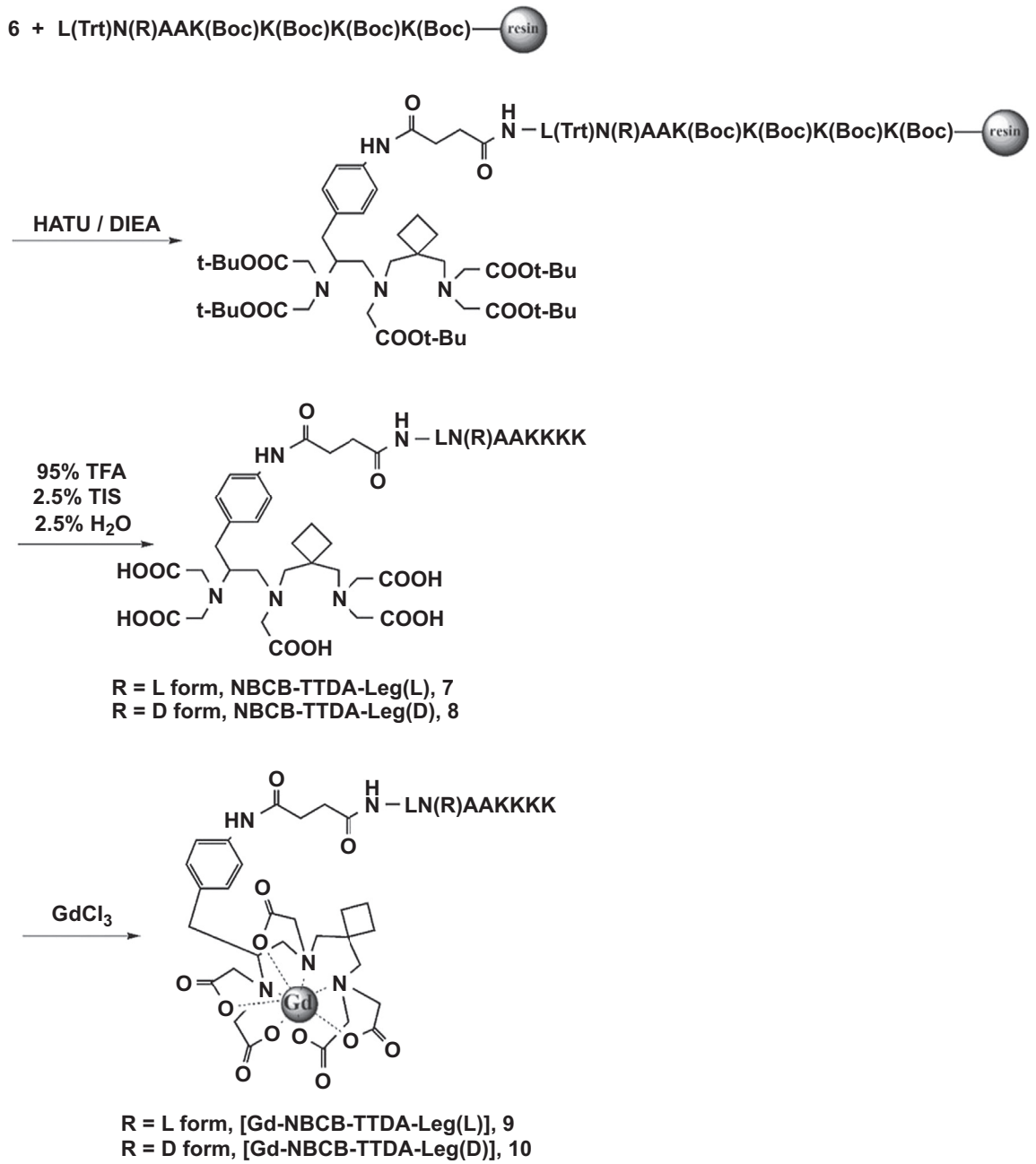

Scheme 1. Synthetic scheme of [Gd-NBCB-TTDA-Leg(L)] and control contrast agent ([Gd-NBCB-TTDA-Leg(D)]).

(2.5 mL) was added to a solution of NBCB-COOH-5est (**6**; 0.32 g, 0.34 mmol) in NMP (3 mL) and shaken vigorously for 15 min. DIEA/NMP (1 mL, 2 M) was then added to the above mixture for 15 s to activate the ligand. The ligand solution was added to the resin and the resulting mixture was shaken vigorously for 8 h. After the reaction was completed, the cleave reagent (10 mL; TFA : deionized water : TIS = 95: 2.5: 2.5 (v/v)) and the resulting mixture was vigorously stirred for 2 h, washed in CH_2Cl_2 and methanol and filtered. After filtration, TEA was added to the mixture to neutralize remnant TFA and then the solvent was vaporized under reduced pressure. To the residue, cold diethyl ether was added and mixture was centrifuged (1500 rpm) for 5 min to precipitate. The same step was repeated for 3–5 times and the white precipitate obtained was collected and lyophilized using deionized distilled water. The freeze-dried powder was concentrated, diluted in H_2O, purified by HPLC, and lyophilized to yield white powder compound **7** (83.0 mg, 27.0%). ESI-MS: *m/z* calculated: 1533.77, found: 1533.69 $[M + H]^+$. The control probe (NBCB-TTDA-Leg(D)) was synthesized by following the steps as mentioned for NBCB-TTDA-Leg(L) by using Leg(D) as a control peptide substrate with yield of compound **8** (86.4 mg, 28.1%). ESI-MS: *m/z* calculated: 1533.77, found: 1534.22 $[M + H]^+$.

2.2.2. Preparation of [Gd-NBCB-TTDA-Leg(L)] (*9*) and [Gd-NBCB-TTDA-Leg(D)] (*10*)

The ligand (NBCB-TTDA-Leg(L)) was dissolved in deionized water (5 mL) and the pH was adjusted to 5.5–6.5 using sodium hydroxide. $GdCl_{3(aq)}$ (510.7 μL, 94.6 mM) was then added to the above solutions and stirred at 25 °C for 72 h. The completion of complex formation was confirmed by xylenol orange test. The solution was filtered and lypophilized to give the white powders complex **9**. The purity of [Gd-NBCB-TTDA-Leg(L)] was determined by HPLC and the identity was confirmed by mass spectrometry. ESI-MS: *m/z* calculated: 1685.98, found: 1685.75 $[M + H]^+$. Complex **10** ([Gd-NBCB-TTDA-Leg(D)]) was prepared using the same procedure as mentioned for [Gd-NBCB-TTDA-Leg(L)] by utilizing NBCB-TTDA-Leg(D) (78 mg, 0.051 mmol) as the control ligand and $GdCl_{3(aq)}$ (510.7 μL, 94.6 mM) as the reaction precursors. The purity of [Gd-NBCB-TTDA-Leg(D)] was determined by HPLC (Fig. S1†) and the identity was confirmed by mass spectrometry. ESI-MS: *m/z* calculated: 1685.98, found: 1686.66 $[M + H]^+$.

2.2.3. Syntheses of CyTE777-Leg(L)-CyTE807 (*13*) and CyTE777-Leg(D)-CyTE807 (*14*)

In a separated vial, CyTE777 (446 mg, 0.57 mmol) and HOBT (77.2 mg, 0.57 mmol) were dissolved in DMF (5 mL) and cooled to 0 °C. DCC (116.9 mg, 0.57 mmol) was added and dissolved by stirring. The solution was then warmed to room temperature and allowed to stand for 24 h after which it was added to the legumain peptide substrate (Leg(L)). The side chain protection group (ivDde) on (L)-Leg was removed by 2% hydrazine in DMF. In a separated vial, CyTE807 (453 mg, 0.57 mmol) and HOBT (77.2 mg, 0.57 mmol) were dissolved in DMF (5 mL) and cooled to 0 °C. To this, DCC (116.9 mg, 0.57 mmol) was added and dissolved by gentle stirring. The solution was warmed to the room temperature and allowed to stand for 24 h after which it was added to the solution. When the reaction was completed, the peptide solution was removed. The resin was washed in DMF and methanol, and dried under vacuum. The cleave reagent (10 mL; TFA : deionized water : TIS = 95 : 2.5 : 2.5 (v/v)) were added to the resin, and N_2 was bubbled through the mixture for 2.0 h. After removing resin, CyTE777-Leg(L)-CyTE807 (**13**) was precipitated in ice-cold diethyl ether and centrifuged (1500 rpm) for 5 min CyTE777-Leg(L)-CyTE807 was concentrated, diluted in H_2O, purified by HPLC (Fig. S2†), and lyophilized to yield green powder compound **13** (229.6 mg, 42.3%). MOLDI-TOF-MS: *m/z* calculated: 2441.17, found: 2440.92 $[M - H]^+$. CyTE777-Leg(D)-CyTE807 (**14**) was prepared using the same procedure as mentioned for compound **13** by utilizing Leg(D) as control peptide substrate. The yield of compound **14** was found to be 229.6 mg (47.8%). MOLDI-TOF-MS: *m/z* calculated: 2441.17, found: 2440.74 $[M - H]^+$.

2.3. Luminescent method for establishing solution hydration state

Luminescence lifetime data was obtained for the Eu(III) complex to determine the number of inner-sphere water molecules in the aqueous solution [21–23]. The luminescence lifetime (s) has been determined in both H_2O and D_2O. The complex containing the number of inner-sphere water was calculated by equations (1) and (2) [28,[36]]

$$q = A\left[1/\tau_{H_2O} - 1/\tau_{D_2O}\right] \quad A = 1.05 \tag{1}$$

$$q = \left(\left[1/\tau_{H_2O} - 1/\tau_{D_2O}\right] - 0.25\right) \times 1.2 \tag{2}$$

where q is the number of water molecules bound to metal ions, τ_{H_2O} luminescence half-life in water solution and τ_{D_2O} is the luminescence half-life in deuterium oxide solution.

2.4. Relaxivity (r_1) measurement

To study the effect of legumain on the longitudinal relaxation time (T_1) of [Gd-NBCB-TTDA-Leg(L)] and the control contrast agent ([Gd-NBCB-TTDA-Leg(D)]), T_1 values were measured in the presence and absence of legumain and HSA, respectively. All the T_1 values were measured using a 20 MHz relaxometer operating at 37.0 ± 0.1 °C. Before each measurement, the relaxometer was tuned and calibrated. The T_1 values were plotted against the concentration of agents, to get six data points, respectively. Furthermore, the values of r_1 were determined from the slope of six data points generated by an inversion-recovery pulse sequence.

2.5. Cell lines and animal model

Legumain-expressing 3T3 (legumain$^+$) cell line was a 3T3 cell line transfected with legumain cDNA. CT-26 (legumain$^+$) (murine colon carcinoma cells), 3T3, and legumain-expressing 3T3 (legumain$^+$) cell lines were cultured in Dulbecco's minimal essential medium supplemented with 10% bovine serum, penicillin (100 μg/mL) and streptomycin (100 μg/mL) with 5% CO_2 at 37 °C. Nude mice (5 weeks old, male) were purchased from the National Laboratory Animal Center (Taipei, Taiwan). Animal experiments were performed in accordance with the institutional guidelines. CT-26 (legumain$^+$) cells (10^6 cells) in PBS (100 μL) with equal volume of matrigel were subcutaneously injected into nude mice ($n = 4$) and used for *in vivo* studies. Cells were injected into the right lateral thigh of the mice. MR imaging was performed two weeks after tumor implantation, at which time the tumors were measured approximately 500 mm^3 in volume.

2.6. Cell cytotoxicity

CT-26 and 3T3 cell lines (10^5 cells) were seeded to the 96-well plates and incubated for 24 h, respectively. Then, [Gd-NBCB-TTDA-Leg(L)], [Gd-NBCB-TTDA-Leg(D)], CyTE777-Leg(L)-CyTE807, and CyTE777-Leg(D)-CyTE807 (each in the range

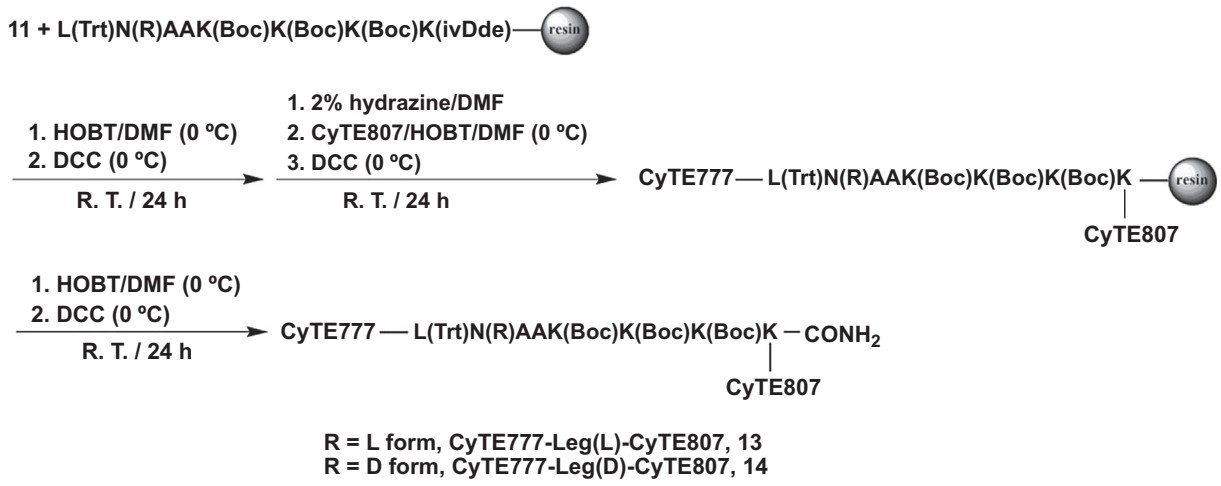

Scheme 2. Synthetic scheme of NIR fluorescent probe (CyTE777-Leg(L)-CyTE807) and control probe (CyTE777-Leg(D)-CyTE807).

Table 1
q values of [Eu-NBCB-TTDA-Leg(L)], [Eu(NBCB-TTDA)]$^{2-}$, and [Eu(BzCB-TTDA)]$^{2-}$.

Compounds	q[b]	q[c]
[Eu-NBCB-TTDA-Leg(L)]	1.19 ± 0.01	1.06 ± 0.01
[Eu(NBCB-TTDA)]$^{2-}$	1.31 ± 0.03	1.20 ± 0.04
[Eu(BzCB-TTDA)]$^{2-}$[a]	1.26 ± 0.02	1.14 ± 0.03

[a] Data were obtained from Ref. [38].
[b] q value obtained using equation (1).
[c] q value obtained using equation (2).

of 0.01–10 μM) were added to the wells. After incubated for 24 h, the supernatant was removed and the cells washed three times in PBS. Cell viability was estimated using the 3-(4,5-dimethylthiazol-2-yl)-2,5-diphenyltetrazolium bromide (MTT) conversion test. MTT (50 μL) solution was added to each well for 2 h, each well was then treated with dimethyl sulfoxide (50 μL) and measured by an ELISA reader at the absorption wavelength set at 570 nm. The data represent the average of sixteen wells. The viability of untreated cells was assumed to be 100%.

2.6.1. In vitro MR imaging study

For the enzymatic cleavage, the MR images of [Gd-NBCB-TTDA-Leg(L)] and control contrast agent ([Gd-NBCB-TTDA-Leg(D)]) were recorded in the presence and absence of legumain and HSA, respectively. All the MR images were obtained by using T_1-weighted (TR/TE = 100/10 ms) two-dimensional spin-echo sequence and the contrast enhancement (%) was calculated by the following equation (3)

$$\text{Enhancement}(\%) = (SI_{\text{post}} - SI_{\text{pre}})/SI_{\text{pre}} \times 100 \quad (3)$$

where SI_{post} is the value of signal intensity of [Gd-NBCB-TTDA-Leg(L)] or control contrast agent ([Gd-NBCB-TTDA-Leg(D)]) with cells and SI_{pre} is the value of signal intensity of [Gd-NBCB-TTDA-Leg(L)] or control contrast agent ([Gd-NBCB-TTDA-Leg(D)]) alone.

2.7. In vitro optical imaging study

CyTE777-Leg(L)-CyTE807 and the control probe (CyTE777-Leg(D)-CyTE807) were prepared with various concentrations (0.31, 0.63, 1.25, and 2.50 μM). The cell lysates of legumain-expressing 3T3 (legumain$^+$) or 3T3 cells (10^5 cells each) were incubated with CyTE777-Leg(L)-CyTE807 and the control probe for 30 min at 37 °C. All samples were scanned at wavelength of excitation 745 nm and emission 820 nm. The contrast enhancement (%) was calculated by equation (3) by considering SI_{post} is the value of signal intensity of CyTE777-Leg(L)-CyTE807 or the control probe (CyTE777-Leg(D)-CyTE807) with cells and SI_{pre} is the value of signal intensity of CyTE777-Leg(L)-CyTE807 or the control probe (CyTE777-Leg(D)-CyTE807) alone.

2.8. In vivo MR imaging study

Nude mice bearing CT-26 (legumain$^+$) tumors were studied by MR imaging when the subcutaneous tumor xenografts reached approximately 500 mm^3. A solution of [Gd-NBCB-TTDA-Leg(L)] (0.1 mmol/kg) was injected via the tail veins. The MR imaging of pentobarbital-anesthetized mice was performed every 10 min for 1 h, using 7.0-T Biospec MR scanner with a volume coil used as radio frequency transmitter and receiver. All animals were scanned using a T_1-weighted fast spin-echo sequence (TR/TE/flip angle = 400/15/10°) for imaging and the corresponding contrast enhancement (%) was calculated by equation (3) by considering SI_{post} is the value of signal intensity for [Gd-NBCB-TTDA-Leg(L)] or the control contrast agent [Gd-NBCB-TTDA-Leg(D)] targeted on tumor cells, and SI_{pre} is the value of signal intensity before [Gd-NBCB-TTDA-Leg(L)] or the control contrast agent [Gd-NBCB-TTDA-Leg(D)] injection.

2.9. In vivo optical imaging study

For the optical imaging experiments, tumor-bearing nude mice were injected via tail veins with CyTE777-Leg(L)-CyTE807 and the control probe (CyTE777-Leg(D)-CyTE807) (2 μmol/kg). Optical imaging was acquired at pre-injection and various time points (0.5, 1, 4, and 24 h) of post-injection. The signal enhancement (%) was calculated by the equation (3), in which SI_{post} is the value of signal intensity for CyTE777-Leg(L)-CyTE807 or the control probe (CyTE777-Leg(D)-CyTE807) targeted on tumor cells, and SI_{pre} is the value of signal intensity before CyTE777-Leg(L)-CyTE807 or the control probe (CyTE777-Leg(D)-CyTE807) injection.

Table 2
Relaxivity (r_1) of [Gd-NBCB-TTDA-Leg(L)], [Gd-NBCB-TTDA-Leg(D)], [Gd(NBCB-TTDA)]$^{2-}$, and [Gd(TTDA)]$^{2-}$, at 20 MHz and 37.0 ± 0.1 °C.

Compounds	pH	Relaxivity (r_1)/mM^{-1} s^{-1}
[Gd-NBCB-TTDA-Leg(L)]	7.4 ± 0.1	4.94 ± 0.03
[Gd-NBCB-TTDA-Leg(D)]	7.4 ± 0.1	4.86 ± 0.02
[Gd(NBCB-TTDA)]$^{2-}$[a]	7.4 ± 0.1	4.28 ± 0.01
[Gd(TTDA)]$^{2-}$[a]	7.4 ± 0.1	3.85 ± 0.03

[a] Data were obtained from Ref. [38].

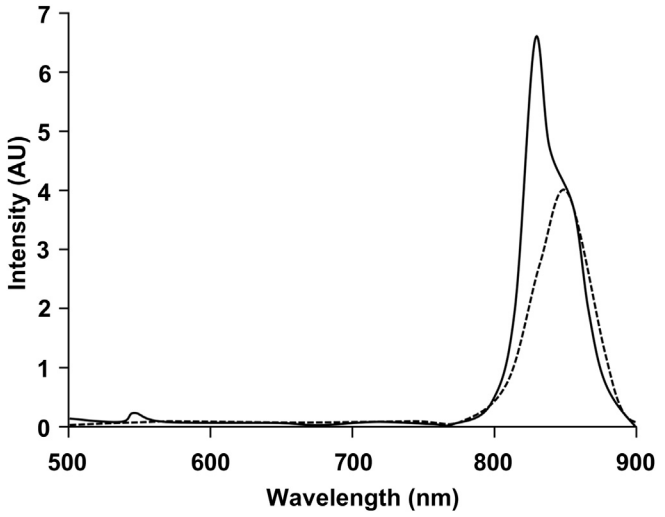

Fig. 2. Fluorescent spectra of CyTE777-Leg(L)-CyTE807 incubated with legumain-transduced 3T3 (legumain$^+$) cell lysate (solid line) and CyTE777-Leg(L)-CyTE807 alone (dotted line) in 0.1 M PBS (excitation: 745 nm).

2.10. Biodistribution study

CyTE777-Leg(L)-CyTE807 and the control probe (CyTE777-Leg(D)-CyTE807) were intravenously injected into tumor-bearing nude mice. Mice were sacrificed 24 h after injection of CyTE777-Leg(L)-CyTE807 and the control probe. Blood, lungs, livers, spleens, hearts, muscles, pancreata, intestines, kidneys, stomachs, bones, skin, and CT-26 (legumain$^+$) tumors were collected and washed (except for blood) in PBS (10 mL). The fluorescent signals of organs were recorded and the results were represented as percentage of injected dose per gram of tissue (% ID/g).

3. Results and discussion

3.1. Syntheses of [Gd-NBCB-TTDA-Leg(L)] and [Gd-NBCB-TTDA-Leg(D)]

In this study, [Gd-NBCB-TTDA-Leg(L)] and the control contrast agent ([Gd-NBCB-TTDA-Leg(D)]) were synthesized for molecular MR imaging by using CB-diamine (**1**), NBPDA (**2**), NBCB (**3**), NBCB-NO_2-5est (**4**), NBCB-NH_2-5est (**5**), NBCB-COOH-5est (**6**), NBCB-TTDA-Leg(L) (**7**), NBCB-TTDA-Leg(D) (**8**), $GdCl_3$, and a legumain-specific peptide substrate or a control peptide that contains D-form asparagine (noncleavable to legumain) as reaction precursors. The reactions involved in the syntheses of ligands and the corresponding gadolinium complexes were given in Schemes S1† and Scheme 1, respectively. All the synthesized compounds were characterized using several techniques such as ^{1}H NMR, ^{13}C NMR, HPLC, and ESI-MS and the data are summarized in respective synthetic part under experimental sections. All the synthesized compounds are relatively stable and soluble in aqueous solutions.

3.2. Syntheses of CyTE777-Leg(L)-CyTE807 and CyTE777-Leg(D)-CyTE807

CyTE777-Leg(L)-CyTE807 was developed as a molecular NIR fluorescent probe and CyTE777-Leg(D)-CyTE807 as a control probe. Schemes S2† and Scheme 2 showed the schematic representation of the syntheses of CyTE777-Leg(L)-CyTE807 and CyTE777-Leg(D)-

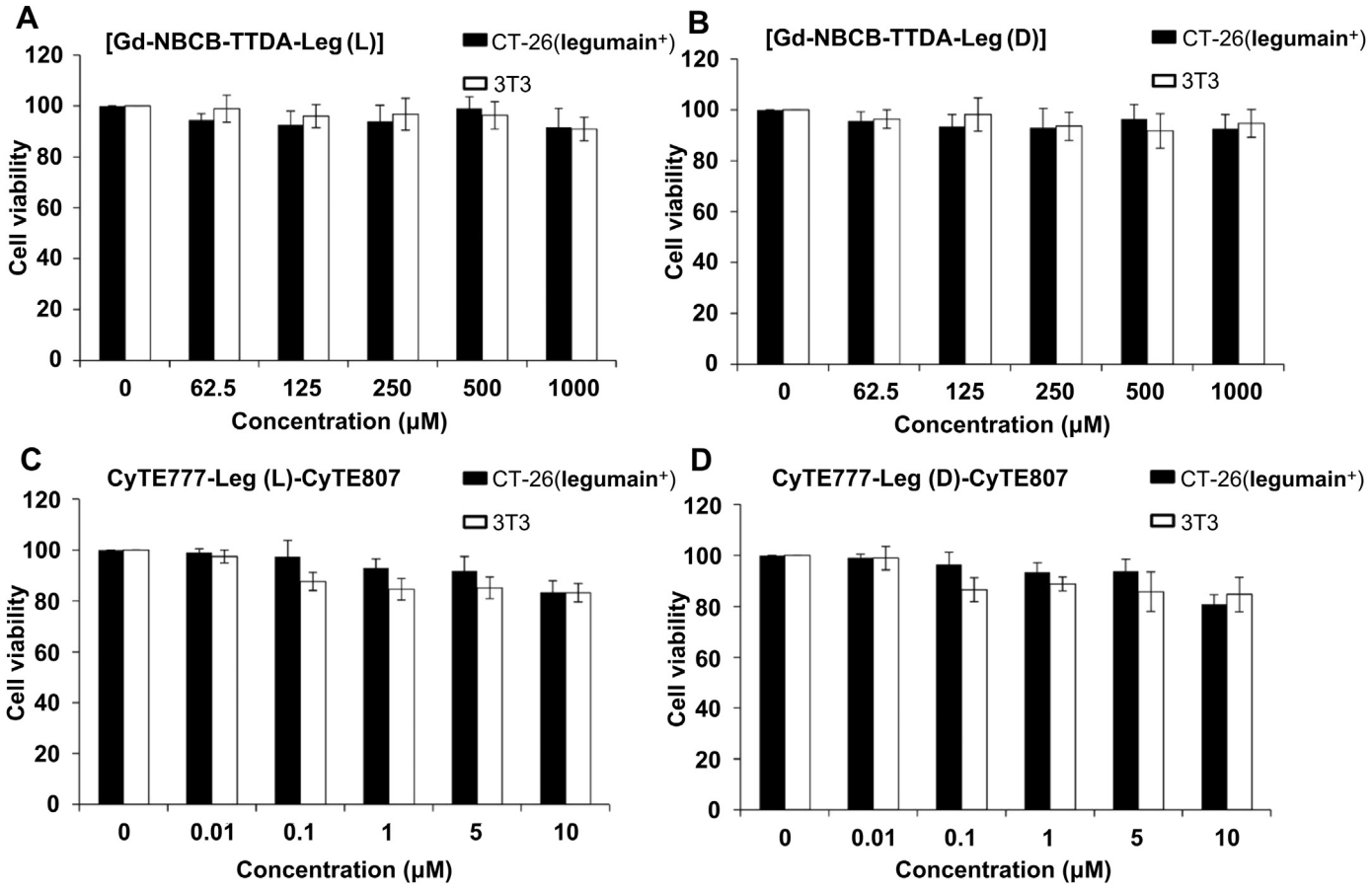

Fig. 3. Cell cytotoxicity of [Gd-NBCB-TTDA-Leg(L)] (A) and [Gd-NBCB-TTDA-Leg(D)] (B), as function of different concentrations (62.5–1000 μM) in MTT assay. Cell cytotoxicity of CyTE777-Leg(L)-CyTE807 (C) and CyTE777-Leg(D)-CyTE807 (D) as function of different concentrations (0.01–10 μM) in MTT assay.

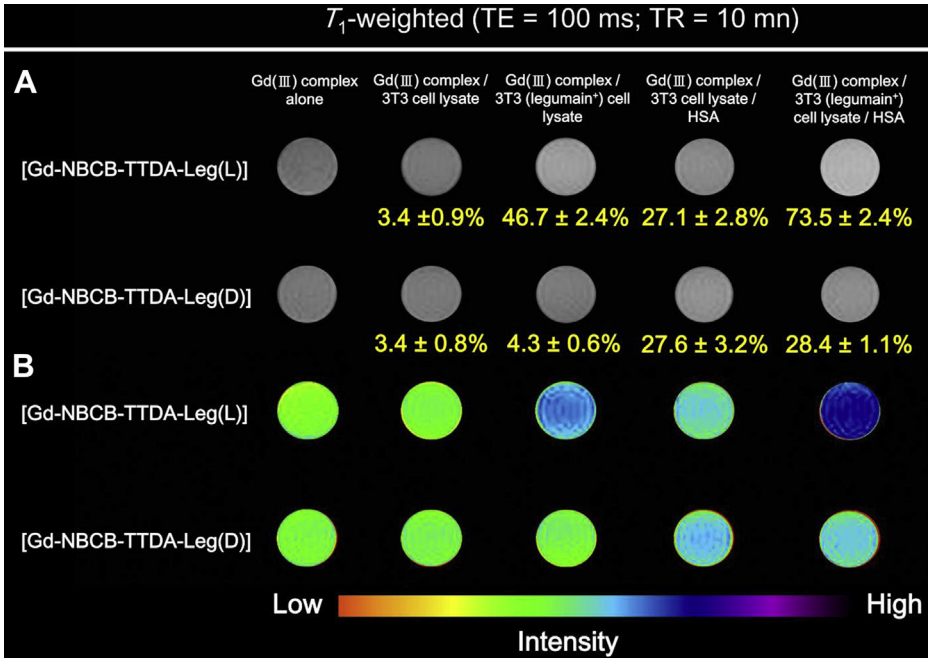

Fig. 4. (A) *In vitro* T_1-weighted MR images of legumain-expressing 3T3 (legumain$^+$) and 3T3 cells treated with 0.25 mM of [Gd-NBCB-TTDA-Leg(L)] and [Gd-NBCB-TTDA-Leg(D)] in the presence and absence of HSA; (B) color-map of MR imaging.

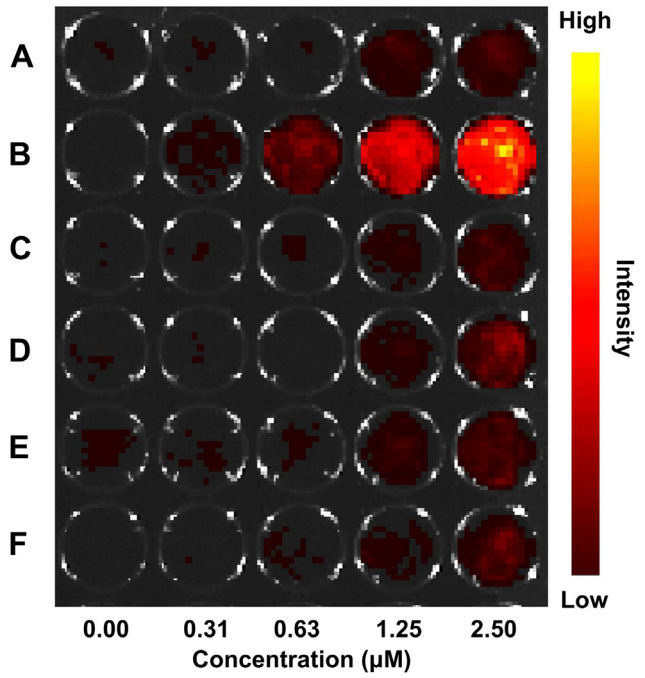

Fig. 5. *In vitro* optical images of legumain-expressing 3T3 (legumain$^+$) and 3T3 cells incubated with CyTE777-Leg(L)-CyTE807, and control probe (CyTE777-Leg(D)-CyTE807) in the presence and absence of HSA; (A) CyTE777-Leg(L)-CyTE807 alone; (B) CyTE777-Leg(L)-CyTE807 incubated with legumain-expressing 3T3 (legumain$^+$) cell lysate; (C) CyTE777-Leg(L)-CyTE807 incubated with 3T3 cell lysate; (D) CyTE777-Leg(D)-CyTE807 alone; (E) CyTE777-Leg(D)-CyTE807 incubated with legumain-expressing 3T3 (legumain$^+$) cell lysate; (F) CyTE777-Leg(D)-CyTE807 incubated with 3T3 cell lysate (excitation: 745 nm; emission: 820 nm).

CyTE807. A previous study has demonstrated that CyTE777 and CyTE807 could be conveniently synthesized in one step [37]. To the Leg(L) substrate sequence, leucine and lysine residues were incorporated at *N*- and *C*-terminal, respectively, for fluorochrome conjugation. Upon complete syntheses of the peptide sequences, the *N*-terminal Fmoc group was removed by piperidine in anhydrous DMF and the amino group was confirmed by Kaiser test [36]. The peptide substrate, which was preactivated by coupling reagent (PyBOP and HOBT), were then coupled to fluorochrome (CyTE777), catalyzed by DCC for 24 h. The crude compounds were washed in methanol and then confirmed for completion of the reaction by Kaiser test. After washed in methanol, CyTE777-Leg(L) was stored at −80 °C to prevent decomposition. The amine-reactive carboxylate group of CyTE807 was further conjugated to the deprotected peptide sequence via the *C*-terminal lysine residue for 24 h. The resin was removed by a mixture of TFA and TIS (10 mL), and the compounds were precipitated by ice-cold diethyl ether. In addition, CyTE777-Leg(D)-CyTE807 was synthesized via the same procedure as mentioned for CyTE777-Leg(L)-CyTE807 by using Leg(D) as a peptide substrate.

3.3. Assessment of hydration state

In order to assess the hydration state of Gd(III) complexes, Eu(III) is commonly applied for lifetime measurements because of its emission falls in the visible spectra and its longer emission time. [24–26] The [Eu-NBCB-TTDA-Leg(L)] complex was synthesized and its luminescent time (s) were measured in both water and deuterium oxide upon excitation at 395 nm. The inner-sphere water molecule calculated for the [Eu-NBCB-TTDA-Leg(L)] complex by using equations (1) and (2) and is found to be 1.19 and 1.06, respectively (Table 1). These results indicate that the q value obtained for [Eu-NBCB-TTDA-Leg(L)] fall within the usual range of single hydration. Our measurements are similar to published data that the q value of [Eu-NBCB-TTDA-Leg(L)] is close to those of $[Eu(NBCB\text{-}TTDA)]^{2-}$ and $[Eu(BzCB\text{-}TTDA)]^{2-}$ [38].

3.4. Relaxivity (r_1) study

The relaxivity (r_1) values of [Gd-NBCB-TTDA-Leg(L)], [Gd-NBCB-TTDA-Leg(D)], $[Gd(NBCB\text{-}TTDA)]^{2-}$, and $[Gd(TTDA)]^{2-}$ at 37.0 ± 0.1 °C are shown in Table 2. The relaxivity values obtained for [Gd-NBCB-TTDA-Leg(L)], [Gd-NBCB-TTDA-Leg(D)], $[Gd(NBCB\text{-}TTDA)]^{2-}$, and $[Gd(TTDA)]^{2-}$ fall within the usual range that corresponds to single hydration (Table 1). The relaxivity of [Gd-NBCB-TTDA-Leg(L)] is similar to that of [Gd-NBCB-TTDA-Leg(D)], and slightly higher than those of $[Gd(NBCB\text{-}TTDA)]^{2-}$ and $[Gd(TTDA)]^{2-}$ likely due to conjugation of the legumain-specific peptide substrate or control peptide thus reduces the tumbling rate and enhances relaxivity [28,[38]].

3.5. Fluorescent study of legumain-induced peptide cleavage of CyTE777-Leg(L)-CyTE807

The NIR fluorescent probe (CyTE777-Leg(L)-CyTE807) was created by conjugating two NIR fluorochromes (CyTE777 and CyTE807) to Leg(L). The emission maxima of CyTE777-Leg(L)-CyTE807, CyTE777, and CyTE807 were 840, 820, and 840 nm, respectively (Fig. 2 and S3†). The fluorescent signals of CyTE777 moiety was completely quenched by CyTE807 resulting from a combination of static quenching and FRET mechanisms [39]. To examine the effect of peptide cleavage by legumain, CyTE777-Leg(L)-CyTE807 was incubated with legumain-transduced 3T3 cell lysate for 0.5 h and then its emission recorded. As shown in Fig. 2, cleavage of the Leg(L) substrate occurred as a consequence of the specific substrate recognition by legumain-induced hydrolysis of asparaginyl bond (Leu–Asn bond) on the legumain peptide substrate. This cleavage induced a slight wavelength shift from 840 nm to 820 nm as compared with the emission from probes without incubation in 3T3 (legumain$^+$) cell lysate. These results indicated that CyTE777-Leg(L)-CyTE807 could be recognized by legumain. Two fluorochromes (CyTE777 and CyTE807) connected by a peptide is expected to quench fluorescent emission by one of the dyes. Cleavage of peptide substrate increased the distance between these two fluorochromes, and revealed the fluorescence emission previously quenched. These results demonstrate that CyTE777-Leg(L)-CyTE807 is recognized specifically on the cleavage site by legumain.

3.6. Cell cytotoxicity

Cytotoxicity is an important parameter for applying the imaging agents in biomedical studies. We used MTT assay to evaluate cytotoxicity of [Gd-NBCB-TTDA-Leg(L)], [Gd-NBCB-TTDA-Leg(D)], CyTE777-Leg(L)-CyTE807, and CyTE777-Leg(D)-CyTE807 to CT-26 (legumain$^+$) and 3T3 cell lines. As shown in Fig. 3, [Gd-NBCB-TTDA-Leg(L)], [Gd-NBCB-TTDA-Leg(D)], CyTE777-Leg(L)-CyTE807 and CyTE777-Leg(D)-CyTE807 displayed low cytotoxicity even at high concentrations of the probes.

3.7. In vitro MR imaging

To further determine the potential utility of [Gd-NBCB-TTDA-Leg(L)], *in vitro* MR imaging studies were performed and the contrast enhancements (%) calculated using the equation (3). Contrast enhancements after incubation with 3T3 or legumain-expressing 3T3 (legumain$^+$) cell lysats in the presence and absence of HSA, attained 3.4 ± 0.9%, 46.7 ± 2.4%, 27.1 ± 2.8%, and 73.5 ± 2.4%, respectively for

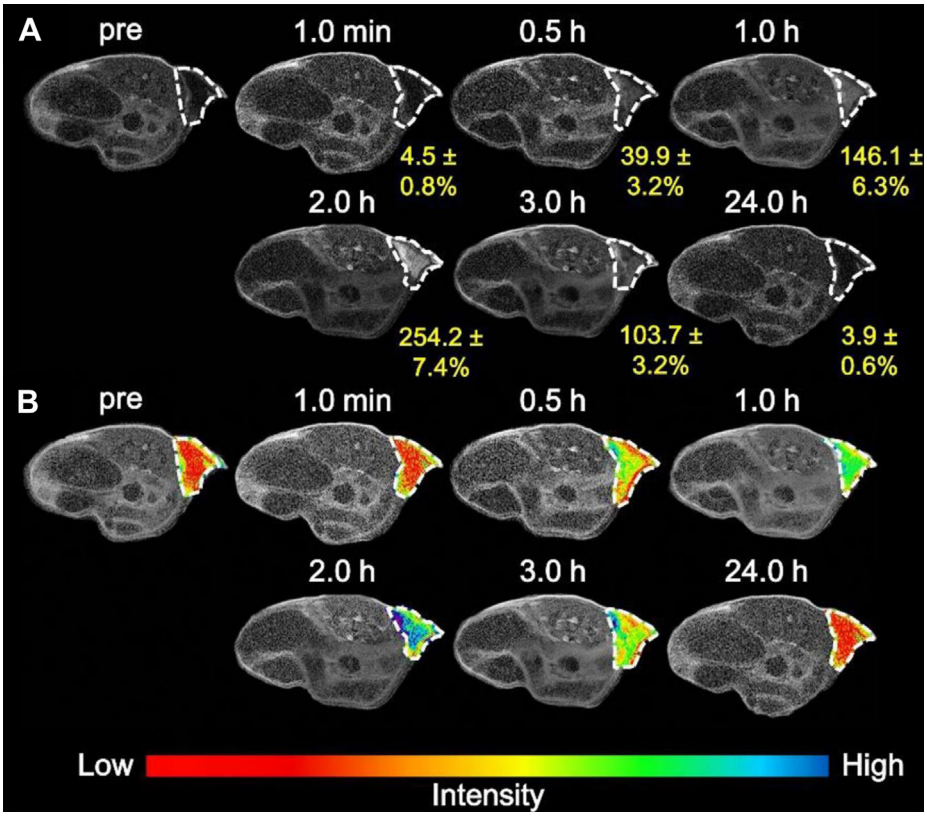

Fig. 6. *In vivo* T_1-weighted MR images of mice bearing CT-26 (legumain$^+$) xenografts pre- and post-injection of [Gd-NBCB-TTDA-Leg(L)] (0.1 mmol/kg) (A). MR imaging was performed on 7.0-T Biospec MR scanner by fast spin echo pulse sequence (TR/TE = 400/15). (B) Color-map of (A).

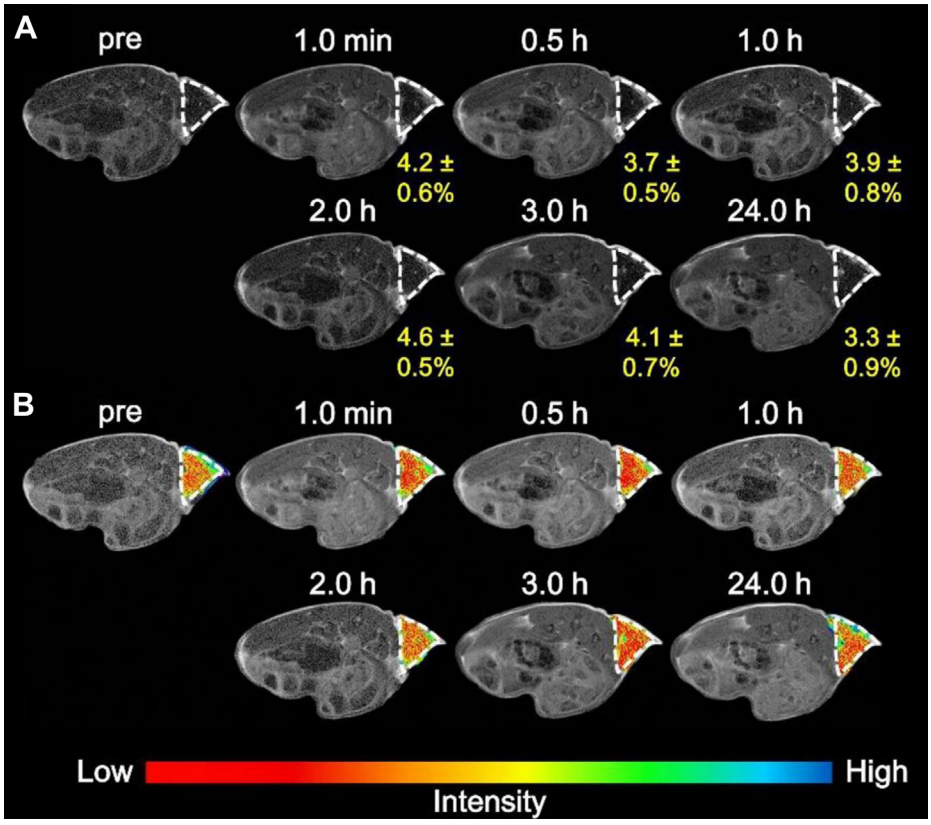

Fig. 7. *In vivo* T_1-weighted MR images of mice bearing CT-26 (legumain$^+$) xenografts pre- and post-injection of [Gd-NBCB-TTDA-Leg(D)] (0.1 mmol/kg) (A). MR imaging was performed on 7.0-T Biospec MR scanner by fast spin echo pulse sequence (TR/TE = 400/15). (B) Color-map of (A).

[Gd-NBCB-TTDA-Leg(L)] (Fig. 4). [Gd-NBCB-TTDA-Leg(L)] showed marked contrast enhancement compared to the control contrast agent ([Gd-NBCB-TTDA-Leg(D)]) (73.5 ± 2.4% vs. 28.4 ± 1.1%, in presence of legumain activity and HSA) [38], likely due to D-form asparagine in the peptide sequence of the control probe renders the peptide resistant to hydrolysis by legumain. These *in vitro* MR imaging results indicate that legumain significantly and specifically increased contrast enhancement of [Gd-NBCB-TTDA-Leg(L)] but not of the control contrast agent [Gd-NBCB-TTDA-Leg(D)].

3.8. In vitro optical imaging

In vitro optical imaging studies were performed with graded concentrations of CyTE777-Leg(L)-CyTE807 and control probe CyTE777-Leg(D)-CyTE807 with the legumain-expressing 3T3 (legumain$^+$) or 3T3 cell lysate. As shown in Fig. 5, signal intensity of CyTE777-Leg(L)-CyTE807 was increased by incubation with legumain-expressing 3T3 (legumain$^+$) cell lysate. In the absence of legumain, signal intensity was slightly increased maybe due to non-specific cleavage to the probe. Only marginal increase in the signal intensity of control probe (CyTE777-Leg(D)-CyTE807) was noted when present at high concentrations. These results indicate that CyTE777-Leg(L)-CyTE807 was specifically cleaved by legumain such that self-quench between CyTE777 and CyTE807 was relieved.

3.9. In vivo MR imaging

In vivo MR imaging was carried out for [Gd-NBCB-TTDA-Leg(L)] and the control contrast agent ([Gd-NBCB-TTDA-Leg(D)]). Images were acquired at pre-injection and various time points (1 min, 0.5 h, 1 h, 2 h, 3 h, and 24 h) after injection of contrast agents to nude mice bearing CT26 (legumain$^+$) tumors. The MR images of [Gd-NBCB-TTDA-Leg(L)] and [Gd-NBCB-TTDA-Leg(D)] after intravenous injection were shown in Figs. 6 and 7. The contrast enhancements (%) at CT26 tumors after [Gd-NBCB-TTDA-Leg(L)] injection reached 4.5%, 39.9%, 146.1%, 254.2%, 103.5%, and 3.9%, respectively. In contrast, only slight enhancements (3.9% at 1 h post-injection, and 4.6% at 2 h post-injection) were observed for the control contrast agent [Gd-NBCB-TTDA-Leg(D)]. The relative contrast enhancement were 37.5 (146.1% versus 3.9%, 1 h post-injection) and 55.3 (254.2% versus 4.6%, 2 h post-injection) fold higher with [Gd-NBCB-TTDA-Leg(L)], compared to the control contrast agent. Thus, [Gd-NBCB-TTDA-Leg(L)] maybe an useful contrast agent for *in vivo* MR imaging of legumain-expressing tumors.

3.10. In vivo optical imaging

To investigate the usefulness of CyTE777-Leg(L)-CyTE807, *in vivo* imaging of mice bearing CT-26 (legumain$^+$) tumors was attempted. CyTE777-Leg(L)-CyTE807 or CyTE777-Leg(D)-CyTE807 were intravenously injected into the tumor-bearing nude mice via tail veins. The fluorescent signals were recorded in mice at various time points (0.5 h, 1 h, 4 h, and 24 h) after injection. As demonstrated in Fig. 8, high fluorescent intensities were observed in the tumors for the mice treated with CyTE777-Leg(L)-CyTE807 (5.23×10^9 photons/min at 0.5 h and 3.34×10^9 photons/min at 24 h post-injection). Furthermore, fluorescent signal persisted in CT-26 (legumain$^+$) tumor over 24 h. On the contrary, minimal

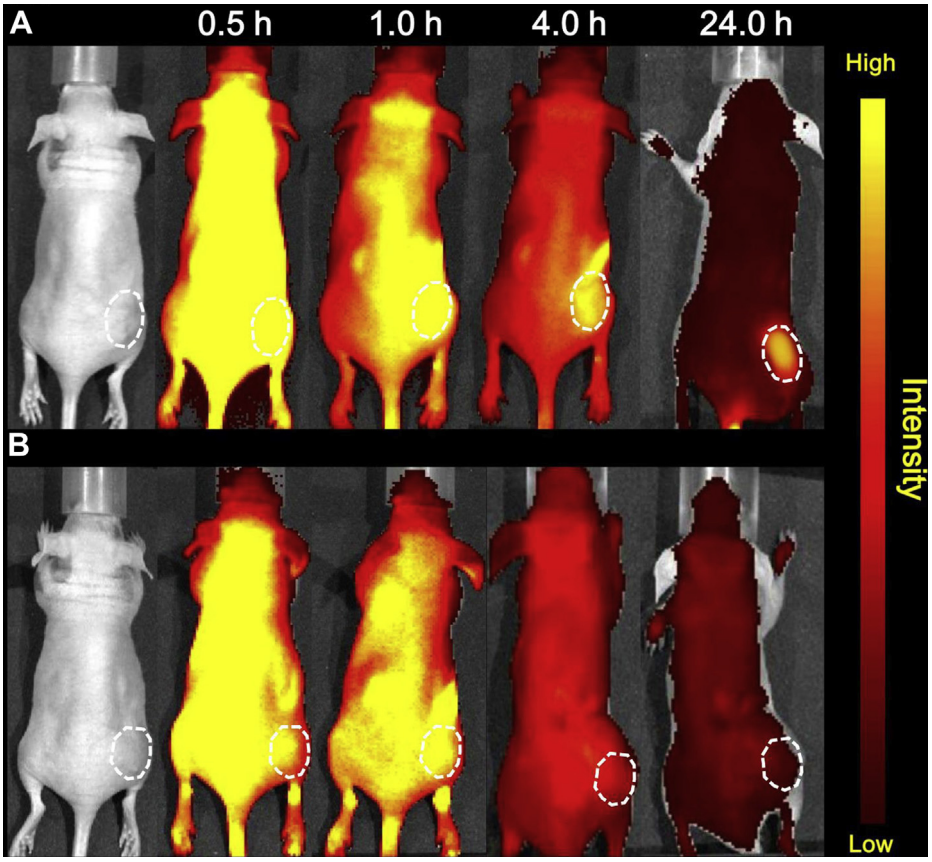

Fig. 8. *In vivo* NIR fluorescence images of CyTE777-Leg(L)-CyTE807 and the control probe (CyTE777-Leg(D)-CyTE807). Mice bearing CT-26 (legumain$^+$) tumor xenograft were injected CyTE777-Leg(L)-CyTE807 (2 μmol/kg) (A) and CyTE777-Leg(D)-CyTE807 (2 μmol/kg) (B). Optical images were acquired pre-injection, 0.5 h, 1 h, 4 h, and 24 h post injection. (excitation: 745 nm; emission: 820 nm).

fluorescent signal was found in the tumors for the mice treated with CyTE777-Leg(D)-CyTE807 (4.98×10^9 photons/min at 0.5 h and 0.22×10^9 photons/min at 24 h, Fig. 8B). The relative fluorescent enhancements were 1.1 fold higher at 0.5 h and 15.2 fold higher at 24 h post-injection with CyTE777-Leg(L)-CyTE807 injection. These results indicate that CyTE777-Leg(L)-CyTE807 is a specific optical imaging probe for legumain-expressing tumors.

3.11. Biodistribution study

The biodistributions of CyTE777-Leg(L)-CyTE807 and control probe (CyTE777-Leg(D)-CyTE807) were examined. CT-26 (legumain$^+$) tumor and other organs were excised and subjected to optical imaging at 24 h post-injection of CyTE777-Leg(L)-CyTE807 or CyTE777-Leg(D)-CyTE807. As shown in Fig. 9, marked fluorescent intensities of CyTE777-Leg(L)-CyTE807 treated mice were noted in CT-26 (legumain$^+$) tumors, livers, and kidneys (5.89×10^9 photons/min, 1.28×10^{10} photons/min, and 1.59×10^9 photons/min, respectively) whereas moderate intensities were detected in skin, pancreata, bones, stomachs, and spleens. Signal percentage per dose gram (% ID/g) for CT-26 (legumain$^+$) tumors, livers, and kidneys were 18.3%, 21.2%, and 7.2%, respectively. On the other hand, fluorescent signals of CyTE777-Leg(D)-CyTE807 treated mice was observed in CT-26 (legumain$^+$) tumors and livers (9.99×10^8 photons/min and 1.62×10^9 photons/min, Fig. 10B). The corresponding % ID/g values for tumors and livers were 1.6% and 26.1% (Fig. 10C). These results clearly demonstrate that CyTE777-Leg(L)-CyTE807 can effectively and specifically accumulate in tumors that over-expresses legumain.

4. Conclusion

In summary, a MRI contrast agent ([Gd-NBCB-TTDA-Leg(L)]) and a NIR fluorescent probe (CyTE777-Leg(L)-CyTE807) were successfully developed. Legumain-mediated cleavage of the substrate peptide increases contrast enhancements or fluorescent intensity of the respective probes. Our data indicate that the contrast agent

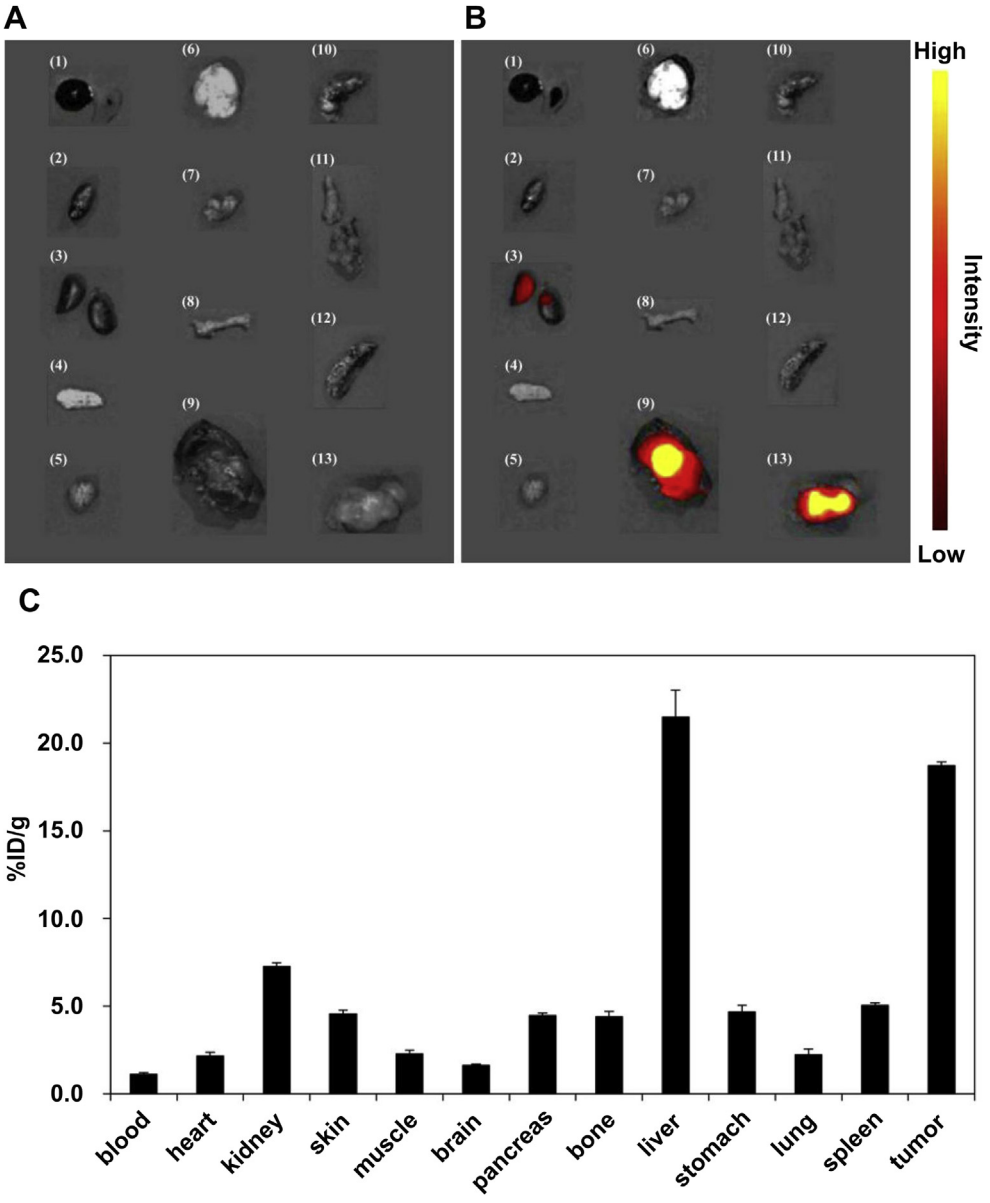

Fig. 9. *In vivo* fluorescent images of dissected organs of mice bearing CT-26 (legumain$^+$) tumors, sacrificed 24 h after intravenous injection of CyTE777-Leg(L)-CyTE807 (20 nmol) (excitation: 745 nm; emission: 820 nm). (A) White light image ((1) blood, (2) heart, (3) kidney, (4) skin, (5) muscle, (6) brain, (7) pancreas, (8) bone, (9) liver, (10) stomach, (11) lung, (12) spleen, (13) CT-26 (legumain$^+$) tumor); (B) near-infrared fluorescence images; (C) quantitative fluorescent intensities of dissected organs of the mice.

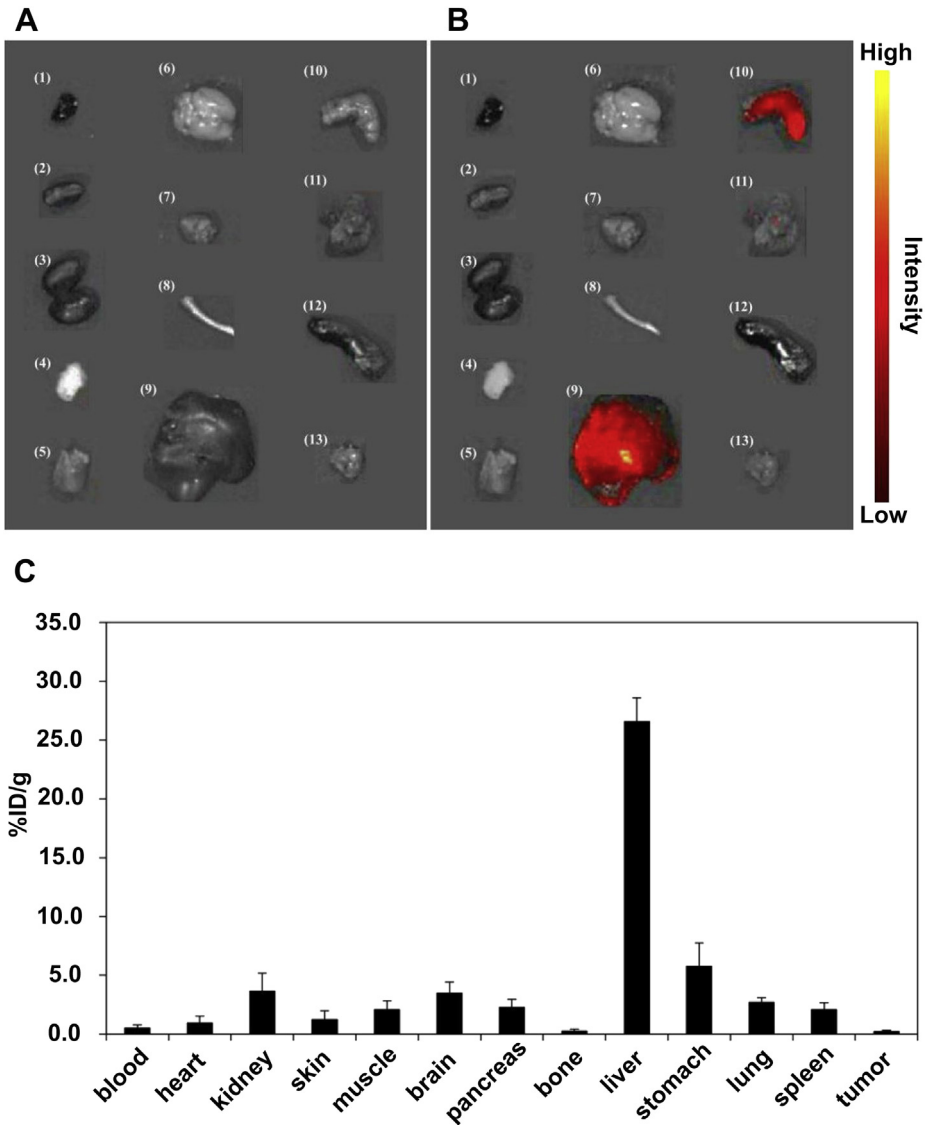

Fig. 10. *In vivo* fluorescent images of dissected organs of the mouse bearing CT-26 (legumain^{+}) tumors, sacrificed 24 h after intravenous injection of CyTE777-Leg(D)-CyTE807 (20 nmol) (excitation: 745 nm; emission: 820 nm). (A) White light image ((1) blood, (2) heart, (3) kidney, (4) skin, (5) muscle, (6) brain, (7) pancreas, (8) bone, (9) liver, (10) stomach, (11) lung, (12) spleen, (13) CT-26 (legumain^{+}) tumor); (B) near-infrared fluorescence images; (C) quantitative fluorescence intensities of dissected organs of the mouse.

and the optical probe can specifically and efficiently target legumain-expressing cancers *in vivo*. Potentially, this strategy can be used for *in vivo* imaging of other proteases by changing the substrate peptides in the constructs. This unique development of efficient MRI contrast agent and optical probe may useful for detection of *in vivo* legumain expression in biomedical studies.

Acknowledgments

We are grateful to the National Science Council of Taiwan for financial support under contracts no. NSC 101-2627-M-009-006. This research was particularly supported by “Aim for the Top University Plan” of the National Chiao Tung University and Ministry of Education.

Appendix A. Supplementary data

Supplementary data related to this article can be found online at http://dx.doi.org/10.1016/j.biomaterials.2013.09.100.

References

[1] Voisin P, Ribot EJ, Miraux S, Bouzier-Sore AK, Lahitte JF, Bouchaud V, et al. Use of lanthanide-grafted inorganic nanoparticles as effective contrast agents for cellular uptake imaging. Bioconjug Chem 2007;18:1053–63.
[2] Frullano L, Meade TJ. Multimodal MRI contrast agents. J Biol Inorg Chem 2007;12:939–49.
[3] Kang X, Yang D, Ma P, Dai Y, Shang M, Geng D, et al. Fabrication of hollow and porous structured $GdVO_4$:Dy^{3+} nanospheres as anticancer drug carrier and MRI contrast agent. Langmuir 2013;29:1286–94.
[4] Choy G, O'Connor S, Diehn FE, Costouros N, Alexander HR, Choyke P, et al. Comparison of noninvasive fluorescent and bioluminescent small animal optical imaging. BioTechniques 2003;35:1022–30.
[5] Su ZF, Liu G, Gupta S, Zhu Z, Rusckowski M, Hnatowich DJ. *In vitro* and *in vivo* evaluation of a technetium-99m-labeled cyclic RGD peptide as a specific marker of $\alpha_v\beta_3$ integrin for tumor imaging. Bioconjug Chem 2002;13:561–70.
[6] Haubner R, Kuhnast B, Mang C, Weber WA, Kessler H, Wester HJ, et al. [^{18}F] Galacto-RGD: synthesis, radiolabeling, metabolic stability, and radiation dose estimates. Bioconjug Chem 2004;15:61–9.
[7] Juran S, Walther M, Stephan H, Bergamann R, Stainbach J, Kraus W, et al. Hexadentate bispidine derivatives as versatile bifunctional chelate agents for copper(II) radioisotopes. Bioconjug Chem 2009;20:347–59.
[8] Liu Z, Yan Y, Liu S, Wang F, Chen X. ^{18}F, ^{64}Cu, and ^{68}Ga labeled RGD-bombesin heterodimeric peptides for PET imaging of breast cancer. Bioconjug Chem 2009;20:1016–25.

[9] Zhang H, Schuhmacher J, Waser B, Wild D, Eisenhut M, Reubi JC, et al. Are radiogallium-labelled DOTA-conjugated somatostatin analogues superior to those labelled with other radiometals? Eur J Nucl Med Mol Imaging 2007;34:1198–208.
[10] Liu Z, Li ZB, Cao Q, Liu S, Wang F, Chen XJ. Small-animal PET of tumors with ^{64}Cu-labeled RGD-bombesin heterodimer. J Nucl Med 2009;50:1168–77.
[11] Weissleder R, Mahmood U. Molecular imaging. Radiology 2001;219:316–33.
[12] Xie H, Zhu Y, Jiang W, Zhou Q, Yang H, Gu N, et al. Lactoferrin-conjugated superparamagnetic iron oxide nanoparticles as a specific MRI contrast agent for detection of brain glioma *in vivo*. Biomaterials 2011;32:495–502.
[13] Cheng Z, Thorek DL, Tsourkas A. Gadolinium-conjugated dendrimer nanoclusters as a tumor-targeted T_1 magnetic resonance imaging contrast agent. Angew Chem Int Ed 2010;49:346–50.
[14] Chen X, Conti PS, Moats RA. *In vivo* near-infrared fluorescence imaging of integrin $\alpha_v\beta_3$ in brain tumor xenografts. Cancer Res 2004;64:8009–14.
[15] Kim S, Lim YT, Soltesz EG, De Grand AM, Lee J, Nakayama A, et al. Near-infrared fluorescent type II quantum dots for sentinel lymph node mapping. Nat Biotechnol 2004;22:93–7.
[16] Colak SB, van der Mark MB, Hooft GW, Hoogengraad JH, van der Linden EW, Kuijpers FA. Clinical optical tomography and NIR spectroscopy for breast cancer detection. IEEE J Sel Top Quantum Electron 1999;5:1143–58.
[17] Weissleder R, Ntziachristos V. Shedding light onto live molecular targets. Nat Med 2003;9:123–8.
[18] Weissleder R. A clearer vision for *in vivo* imaging. Nat Biotechnol 2001;19:316–7.
[19] Tung CH. Fluorescent peptide probes for *in vivo* diagnostic imaging. Biopolymers 2004;76:391–403.
[20] Rao J, Dragulescu-Andrasi A, Yao H. Fluorescence imaging *in vivo*: recent advances. Curr Opin Biotechnol 2007;18:17–25.
[21] Artemov D, Mori N, Ravi R, Bhujwalla ZM. Magnetic resonance molecular imaging of the HER-2/neu receptor. Cancer Res 2003;63:2723–7.
[22] Artemov D, Mori N, Okollie B, Bhujwalla ZM. MR molecular imaging of the Her-2/*neu* receptor in breast cancer cells using targeted iron oxide nanoparticles. Magn Reson Med 2003;49:403–8.
[23] Wrensch M, Minn Y, Chew T, Bondy M, Berger MS. Epidemiology of primary brain tumors: current concepts and review of the literature. Neuro-Oncology 2002;4:278–99.
[24] Parsons SL, Watson SA, Steele RJ. Phase I/II trial of batimastat, a matrix metalloproteinase inhibitor, in patients with malignant ascites. Eur J Surg Oncol 1997;23:526–31.
[25] Nelson AR, Fingleton B, Rothenberg ML, Matrisian LM. Matrix metalloproteinases: biologic activity and clinical implications. J Clin Oncol 2000;18:1135–49.
[26] Chiappori AA, Eckhardt SG, Bukowski R, Sullivan DM, Ikeda M, Yano Y, et al. A phase I pharmacokinetic and pharmacodynamic study of s-3304, a novel matrix metalloproteinase inhibitor, in patients with advanced and refractory solid tumors. Clin Cancer Res 2007;13:2091–9.
[27] Beattie GJ, Smyth JF. Phase I study of intraperitoneal metalloproteinase inhibitor BB94 in patients with malignant ascites. Clin Cancer Res 1998;4:1899–902.
[28] Wang YM, Lee CH, Liu GC, Sheu RS. Synthesis and complexation of Gd^{3+}, Ca^{2+}, Cu^{2+} and Zn^{2+} by 3, 6, 10-tri (carboxymethyl)-3, 6, 10-triazadodecanedioic acid. Dalton Trans 1998;24:4113–8.
[29] Lee J, Bogyo M. A bright approach to the immunoproteasome: Development of LMP2/β1i-specific imaging probes. Bioorg Med Chem Lett 2012;22:1340–3.
[30] van Eijk M, Johannes C, van Noorden F, de Groot C. Proteinases and their inhibitors in the immune system. Int Rev Cytol 2003;222:197–236.
[31] Chen JM, Fortunato M, Stevens RA, Barrett AJ. Inhibition of distant caspase homologues by natural caspase inhibitors. Biol Chem 2001;382:777–83.
[32] Shirahama-Noda K, Yamamoto A, Sugihara K, Hashimoto N, Asano M, Nishimura M, Hara-Nishimura I. Biosynthetic processing of cathepsins and lysosomal degradation are abolished in asparaginyl endopeptidase-deficient mice. J Biol Chem 2003;278:33194–9.
[33] Sarandeses CS, Covelo G, Diaz-Jullien C, Freire M. Prothymosin α is processed to thymosin α1 and thymosin α11 by a lysosomal asparaginyl endopeptidase. J Biol Chem 2003;278:13286–93.
[34] Morita Y, Araki H, Sugimoto T, Takeuchi K, Yamane T, Maeda T, et al. Legumain/asparaginyl endopeptidase controls extracellular matrix remodeling through the degradation of fibronectin in mouse renal proximal tubular cells. FEBS Lett 2007;7:1417–24.
[35] Lin YH, Dayananda K, Chen CY, Liu GC, Luo TY, Hsu HS, et al. *In vivo* MR/optical imaging for gastrin releasing peptide receptor of prostate cancer tumor using Gd-TTDA-NP-BN-Cy5. 5. Bioorg Med Chem 2011;19:1085–96.
[36] Kaiser E, Colescott RL, Bossinger CD, Cook PI. Color test for detection of free terminal amino groups in the solid-phase synthesis of peptides. Anal Biochem 1970;34:595–8.
[37] Hilderbrand SA, Kelly KA, Weissleder R, Tung CH. Monofunctional near-infrared fluorochromes for imaging applications. Bioconjug Chem 2005;16:1275–81.
[38] Chang YH, Chen CY, Singh G, Chen HY, Liu GC, Goan YG, et al. Synthesis and physicochemical characterization of carbon backbone modified [Gd(TTDA)(H2O)]$^{2-}$ derivatives. Inorg Chem 2011;50:1275–87.
[39] Johansson MK, Cook RM. Intramolecular dimers: a new design strategy for fluorescence-quenched probes. Chem Eur J 2003;9:3466–71.